DINAME 2019 - Proceedings of the XVIII International Symposium on Dynamic Problems of Mechanics,
M.A. Savi, T.G. Ritto and W.M. Bessa (Editors), ABCM, Buzios, RJ, Brazil, March 10th to 15th, 2019

Numerical analyses of two articulated rigid pipes ejecting fluid and subjected to support excitation

Igor Mancilla Lourenço and Guilherme Rosa Franzini

Offshore Mechanics Laboratory, Escola Politécnica, University of São Paulo, Brazil.

igorml@usp.br
gfranzini@usp.br

Abstract: This work deals with the parametric instability analyses of two articulated rigid pipes (like a double-pendulum) ejecting fluid. The instability of the trivial solution is investigated using the Floquet Theory. Herein, parametric instability is reached by imposing vertical and harmonic motion to the support of the rigid pipes. The linearized equations of motion are derived and curves of instability are obtained for different combinations of parametric excitation amplitude and frequency and for some selected internal flow velocities. Among other findings, the paper reveals that the presence of internal flow significantly affects the regions in the control parameters in which unbounded solutions are obtained.

Keywords: Pipe ejecting fluid, parametric instability, Floquet Theory, linear dynamics

INTRODUCTION

Risers are slender structures commonly employed in the offshore engineering scenario for conveying fluid from the seabed to the floating unit. In addition to the internal flow, other sources of excitation include the external flow (causing, for example, vortex-induced vibrations) and that arisen as a consequence of the motion of the floating unit.

The problem of slender pipes conveying fluid has been studied since the 1960's, when Benjamin (1961) analyzed the stability of a two degrees-of-freedom planar model of a pipe ejecting fluid. In this paper, the author proposed an analytical approach based on the Hamilton's principle for the derivation of the equations of motion. In Paidoussis (1998), the problem of slender structures with axial flow was widely studied.

An alternative approach for deriving a reduced-order model for an inextensible cantilevered pipe conveying fluid was shown in Orsino and Pesce (2018). In the latter reference, the authors proposed a new modular methodology, providing an algorithm in which all the effects due to kinematic constraints can be computed *a posteriori* and using adequate projection operators. The results in this revealed good agreement with the classical solutions presented in Paidoussis (1998). Considering deepwater oil exploration, the analyses of combined effects become important. Orsino et al. (2017,2018) proposed and investigated a non-linear reduced order model for a submerged cantilevered pipe ejecting fluid under vortex-induced vibrations.

In turn, parametric instability occurs when at least one of the parameters of the equation of motion depend explicitly on time. An archetypal problem in which parametric instability is observed is the pendulum with vertical and harmonic motions applied to the support. The textbooks written by Nayfeh and Mook (1979) and Meirovitch (2003) are surveys on the theme. Still considering the pendulum with support excitation, the linear equation of motion is also known as Mathieu's equation. Depending on the combination of amplitude and frequency of the prescribed motion, the trivial solution may be stable (bounded response) or unstable (unbounded solutions). A straightforward way to the check the stability of the trivial solution is by means of the Strutt's diagram. In the riser's context, parametric instability occurs due to the time-dependent normal force associated with the motion of the floating unit.

Motivated by the technological application of a riser conveying fluid and subjected to the parametric instability phenomenon, this paper aims at contributing with the analysis of these combined problems. Even though the technological motivation, the focus here is placed on an extension of the classical Benjamin's problem by including the effects of the parametric instability. Herein, the dynamics of two articulated rigid pipes assembled as a double-pendulum ejecting fluid and subjected to harmonic support excitation is numerically studied. The Floquet Theory is applied aiming at identifying regions in the plane of parameters that govern the support excitation (namely, its amplitude and frequency) in which bounded and unbounded solutions are obtained for different internal flow velocities.

MATHEMATICAL MODEL

Fig. 1 shows the problem herein investigated. The rigid pipes have length L_1 and L_2, mass *per* unit length m and are linked by torsional springs of constant k_1 and k_2. The internal flow has constant velocity U and the fluid has mass *per* unit length M. The vector r_L represents the position of the free end of the pipe and the unit vector $\mathbf{n}$ is tangent to the direction

of pipe 2. The motion applied to the support is given by $y = A\cos(\Omega t)$.

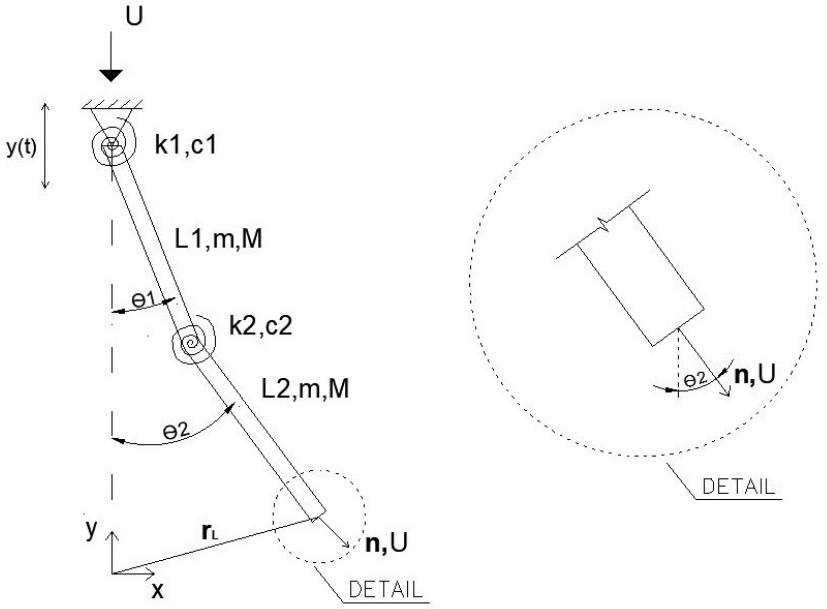

Figure 1 – Model of pipe conveying fluid with support excitation.

The kinetic and potential energies are given by Eqs. 1 and 2.

$$\begin{aligned}T_{Total} =& T_1 + T_2 + T_{f1} + T_{f2} \\ =& \frac{1}{8}L_1^3(m+M)\dot{\theta}_1^2 + \frac{1}{24}L_1^3(m+M)\dot{\theta}_1^2 + \frac{1}{2}L_1^2L_2(m+M)\dot{\theta}_1^2 + \frac{1}{8}L_2^3(m+M)\dot{\theta}_2^2 + \frac{1}{24}L_2^3(m+M)\dot{\theta}_2^2 + \\ &+ \frac{1}{2}L_1(m+M)\dot{y}^2 + \frac{1}{2}L_2(m+M)\dot{y}^2 + \frac{1}{2}(L_1+L_2)MU^2 - \frac{1}{2}L_2^2(m+M)\sin\theta_2\dot{\theta}_2\dot{y} + (L_1+L_2)M\cos\theta_2 U\dot{y} + \\ &+ L_1L_2M\sin(\theta_2-\theta_1)U\dot{\theta}_1 - \frac{1}{2}L_1^2(m+M)\sin\theta_1\dot{\theta}_1\dot{y} + \frac{1}{2}L_1L_2^2(m+M)\cos(\theta_2-\theta_1)\dot{\theta}_1\dot{\theta}_2 - L_1L_2(m+M)\sin\theta_1\dot{\theta}_1\dot{y}\end{aligned} \tag{1}$$

$$\begin{aligned}V_{Total} =& V_1 + V_2 + V_{f1} + V_{f2} + V_{k1} + V_{k2} \\ =& L_1(m+M)g\left(\frac{L_1}{2} - \frac{L_1}{2}\cos\theta_1 - y\right) + L_2(m+M)g\left(L_1 + \frac{L_2}{2} - L_1\cos\theta_1 - \frac{L_2}{2}\cos\theta_2 - y\right) + \frac{1}{2}k_2(\theta_2-\theta_1)^2 + \\ &+ \frac{1}{2}k_1\theta_1^2\end{aligned} \tag{2}$$

Where T_1, T_2 represent the kinetic energy of first and second pipes respectively and T_{f1} and T_{f2} are the kinetic energy of fluid inside the pipes. Following, V_{f1} and V_{f2} are the gravitational potential energy of fluid inside the pipes, V_{k1} and V_{k2} are the elastic potential and V_1 and V_2 are the gravitational potential energy of pipes. The hydrodynamic forces are included in the virtual work of the non-conservative forces δW_n.

$$\delta W_n = \left((\dot{\mathbf{r}}_L + U\mathbf{n}_L).UM\frac{\partial \mathbf{r}_L}{\partial \theta_n}\right)\delta\theta_n \tag{3}$$

The non-linear equations of motion are obtained by substituting Eqs. 1, 2 and 3 into the Euler-Lagrange's equations. As we focus on the use of Floquet Theory, the linearized mathematical model must be considered in the form of Eqs. 4 and 5.

$$\frac{1}{3}L_1^3(m+M)\ddot{\theta}_1 + L_1^2L_2(m+M)\ddot{\theta}_1 + \frac{1}{2}L_1L_2^2(m+M)\ddot{\theta}_2 + (L_1^2MU + c_{1,1})\dot{\theta}_1 + (2L_1L_2MU + c_{1,2})\dot{\theta}_2 +$$
$$+ (k_1+k_2)\theta_1 + \frac{1}{2}L_1^2(m+M)g\theta_1 + L_1L_2(m+M)g\theta_1 - \frac{1}{2}L_1^2(m+M)\theta_1\ddot{y} - L_1L_2(m+M)\theta_1\ddot{y} -$$
$$- L_1MU^2\theta_1 - k_2\theta_2 + L_1MU^2\theta_2 = 0 \quad (4)$$
$$\frac{1}{2}L_1L_2^2(m+M)\ddot{\theta}_1 + \frac{1}{3}L_2^3(m+M)\ddot{\theta}_2 + (c_{2,1})\dot{\theta}_1 + (L_2^2MU + c_{2,2})\dot{\theta}_2 - k_2\theta_1 - \frac{1}{2}L_2^2(m+M)\ddot{y}\theta_2 + k_2\theta_2 +$$
$$+ \frac{1}{2}L_2^2(m+M)g\theta_2 = 0 \quad (5)$$

Where the $c_{i,j}$ are terms associated with linear and proportional structural damping. Now, we define a series of dimensionless quantities as follows:

$$\psi = \frac{L_1}{L_2}, \beta = \frac{6M}{m+M}, \nu = \frac{U}{L_2\Omega}, \kappa_i = \frac{12k_i}{L_2^3(m+M)\Omega^2}, C_{i,j} = \frac{6c_{i,j}}{L_2^3(m+M)\Omega^2},$$

$$\rho = \frac{6g}{L_2\Omega^2}, \Delta = \frac{6A}{L_2}, U^* = \frac{U}{L_2\Omega_1}$$

Using the above definitions, the dimensionless equations are given by:

$$\left(\psi^3 + 3\psi^2\right)\ddot{\theta}_1 + \left(\frac{3}{2}\psi\right)\ddot{\theta}_2 + \left(\beta\nu\psi^2 + C_{1,1}\right)\dot{\theta}_1 + \left(2\beta\nu\psi + C_{1,2}\right)\dot{\theta}_2 + \left(2\beta\nu^2\psi - \kappa_2\right)\theta_2 +$$
$$+ \left(\psi^2\rho + 2\psi\rho + \kappa_1 + \kappa_2 - 2\beta\nu^2\psi + (\psi^2\Delta + 2\psi\Delta)\cos(2\tau)\right)\theta_1 = 0 \quad (6)$$
$$\left(\frac{3}{2}\psi\right)\ddot{\theta}_1 + \ddot{\theta}_2 + (C_{2,1})\dot{\theta}_1 + (\beta\nu + C_{2,2})\dot{\theta}_2 + (-\kappa_2)\theta_1 + (\kappa_2 + \rho + \Delta\cos(2\tau))\theta_2 = 0 \quad (7)$$

U^* being the velocity of the internal flow normalized by first natural frequency of the model filled with fluid at null velocity Ω_1.

NUMERICAL SIMULATIONS AND PRELIMINARY RESULTS

The numerical solutions of Eqs. 6 and 7 are obtained by using Mathematica®. The total integration is π, the period of the parametric excitation and in according to the Floquet Theory. The time-step is chosen automatically by the NDSolve function. The Floquet Theory is applied to identify regions in the plane of dimensionless parameters $\Delta \times \rho$ in which bounded solutions appear. Notice that these mentioned parameters are associated with the frequency and the amplitude of the imposed motion.

Each stability diagram is acquired for particular sets of internal flow velocity, structural damping and dimensionless mass. The results were organized in the groups showed in Tabs. 1, 2 and 3.

The parameters of structural damping, dimensionless mass and internal flow velocity are varying in each situation of analyzes. The Figs. 2, 3 and 4 show the regions of bounded (shaded in black) and unbounded responses as functions of Δ and ρ for four different internal flow velocities (represented by the dimensionless quantity U^*), four different structural damping (represented by the dimensionless quantity ξ) and three different dimensionless masses (represented by the dimensionless quantities β).

All values of U^* are less than critical velocity of stability. The results for the first group are presented in Fig. 2) and show that the increase in U^* and ξ enlarged the region of bounded responses. The diagram associated with the J1 case presents some failures in the region of bounded responses. These failures indicate regions of unbounded responses in the tongues of stability. This effect remain the same when increase dimensionless mass (β) values (see Figs. 3 and 4).

Figure 3 shows the results with $\beta = 0.500$. The increase in U^* expanded the region of bounded solution and gave rise to a sub-region of stability. It is possible to see in diagrams families T. This sub-region appears between the frequencies values corresponding to $\rho = 25.0$ and $\rho = 35.0$ for dimensionless velocity equal to $U^* = 1.389$. With the increase of structural damping (ξ) this sub-region separates of the principal region of stability, create an "island" of bounded response inside the instability region.

Table 1 – Nomenclature of each carry out cases $\beta = 0.200$.

	$\beta = 0.200$			
	$\xi = 0\%$	$\xi = 2\%$	$\xi = 5\%$	$\xi = 10\%$
$U^* = 0.000$	J1	J2	J3	J4
$U^* = 0.347$	K1	K2	K3	K4
$U^* = 0.695$	L1	L2	L3	L4
$U^* = 1.042$	M1	M2	M3	M4
$U^* = 1.389$	N1	N2	N3	N4

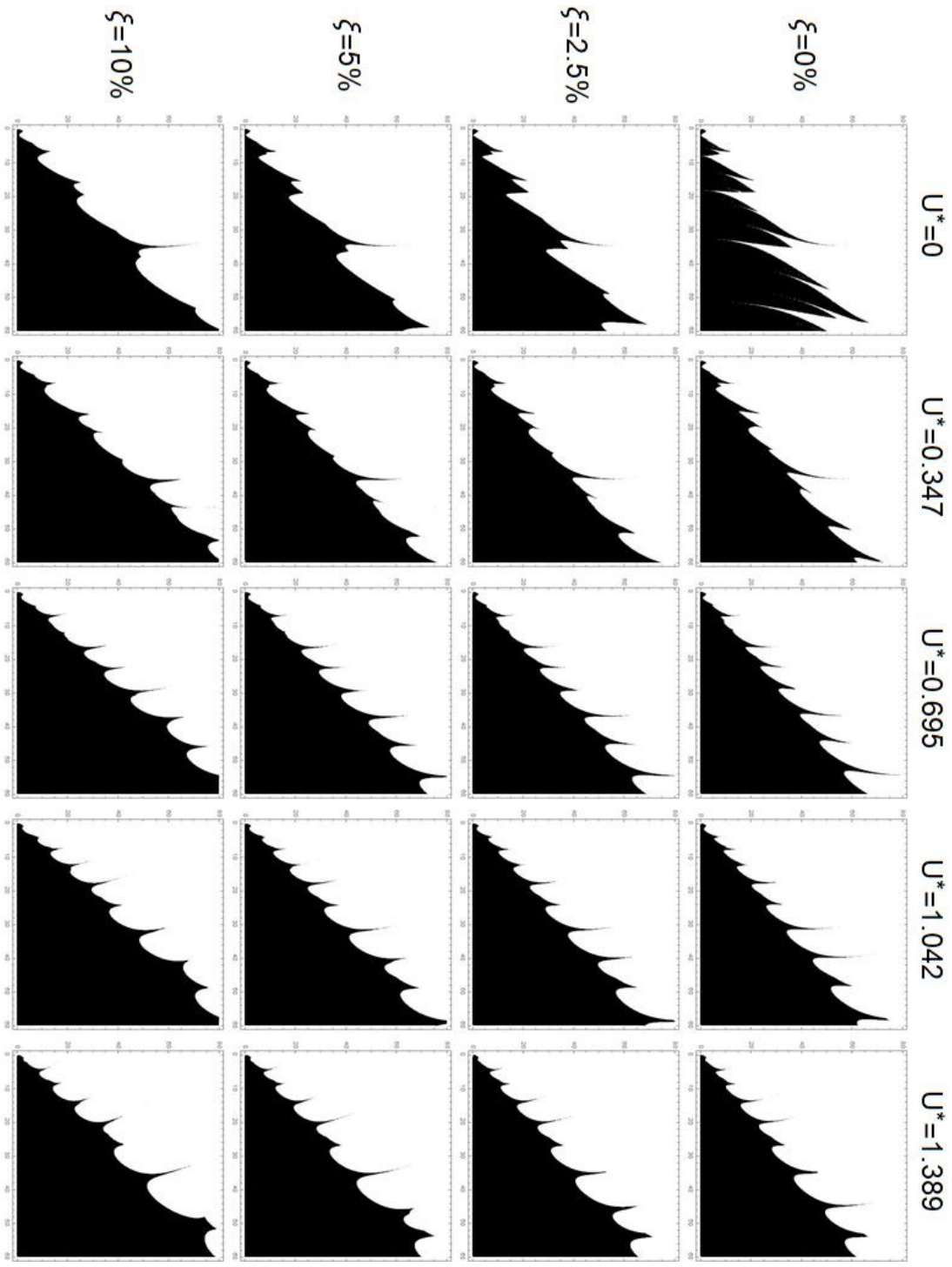

Figure 2 – Qualitative analyses of the stability diagrams for $\beta = 0.200$. Abscissas axis (ρ) varying from 0 to 60 and ordinates axis varying from 0 to 80. Figure rotated 270 degrees.

Table 2 – Nomenclature of each carry out cases $\beta = 0.500$.

	$\beta = 0.500$			
	$\xi = 0\%$	$\xi = 2\%$	$\xi = 5\%$	$\xi = 10\%$
$U^* = 0.000$	O1	O2	O3	O4
$U^* = 0.347$	P1	P2	P3	P4
$U^* = 0.695$	R1	R2	R3	R4
$U^* = 1.042$	S1	S2	S3	S4
$U^* = 1.389$	T1	T2	T3	T4

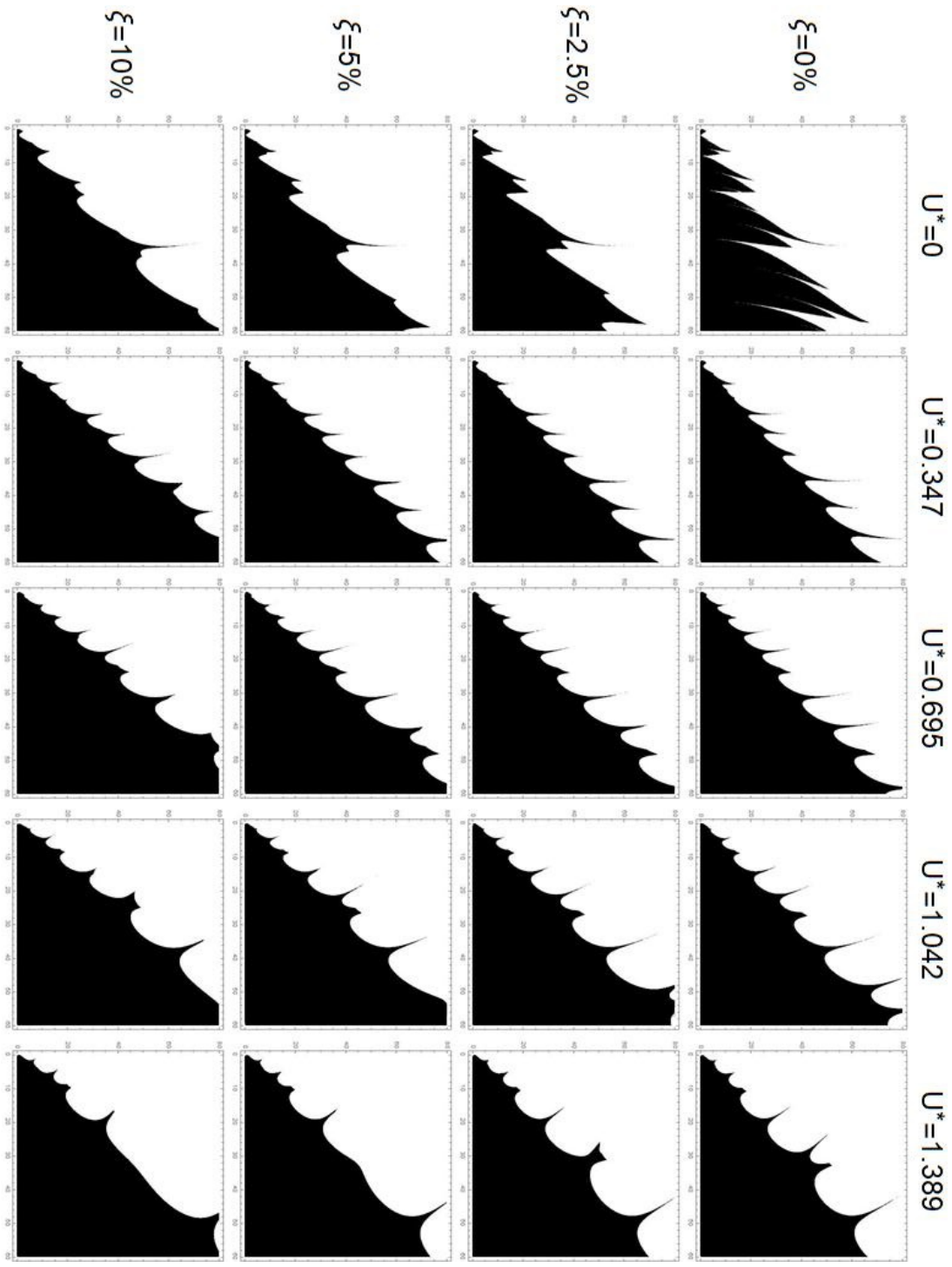

Figure 3 – Qualitative analyses of the stability diagrams for $\beta = 0.500$. Abscissas axis (ρ) varying from 0 to 60 and ordinates axis varying from 0 to 80. Figure rotated 270 degrees.

Table 3 – Nomenclature of each carry out cases $\beta = 0.750$.

	$\beta = 0.750$			
	$\xi = 0\%$	$\xi = 2\%$	$\xi = 5\%$	$\xi = 10\%$
$U^* = 0.000$	U1	U2	U3	U4
$U^* = 0.347$	V1	V2	V3	V4
$U^* = 0.695$	X1	X2	X3	X4
$U^* = 1.042$	Y1	Y2	Y3	Y4
$U^* = 1.389$	Z1	Z2	Z3	Z4

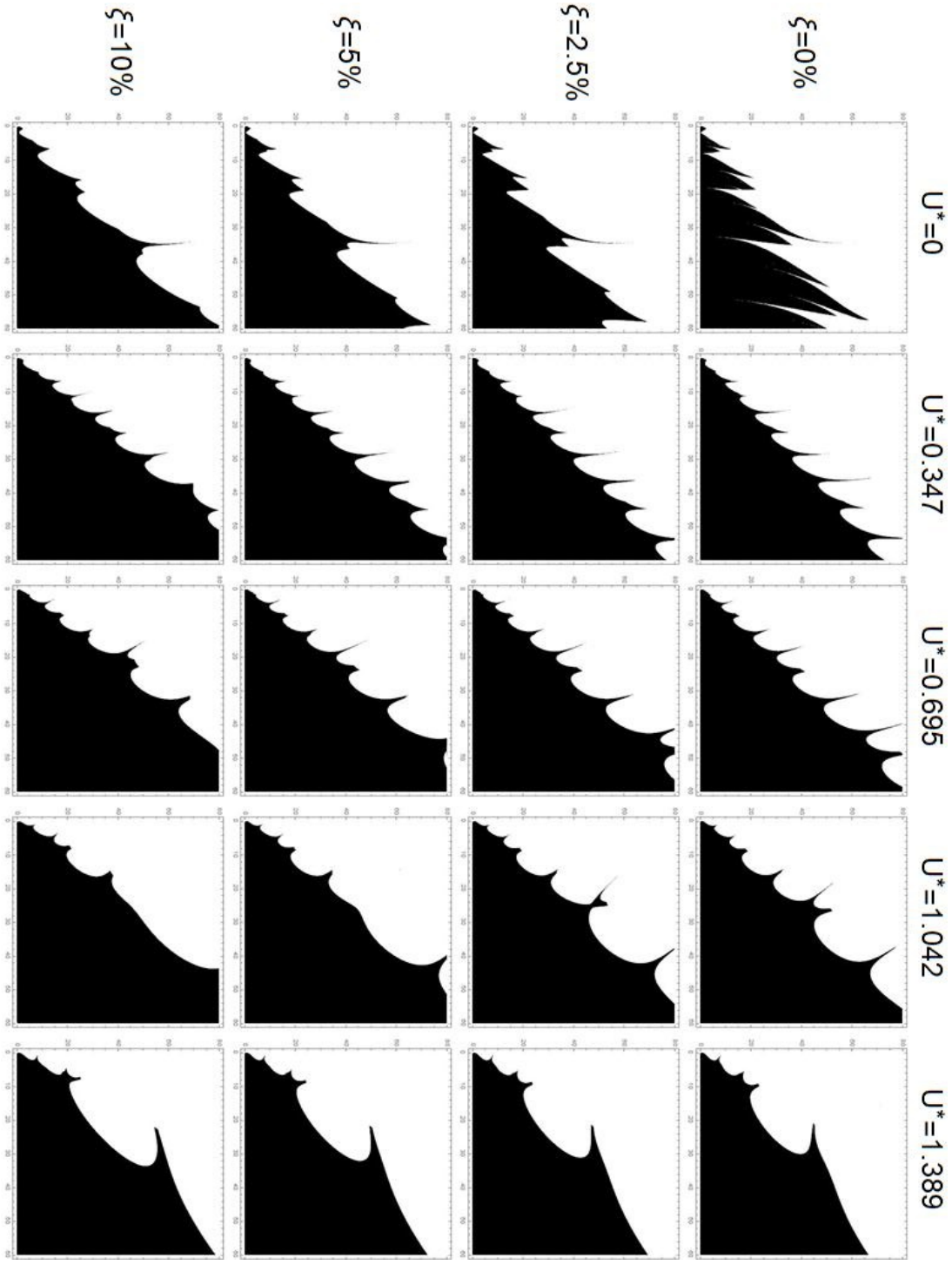

Figure 4 – Qualitative analyses of the stability diagrams for $\beta = 0.750$. Abscissas axis (ρ) varying from 0 to 60 and ordinates axis varying from 0 to 80. Figure rotated 270 degrees.

Figure 4 depicts the stability map for $\beta = 0.750$. For this value of dimensionless mass the sub-region of stability appears from lower values of dimensionless velocity than in the others groups. Additionally, the separation of the sub-region occurs for a lower value of internal flow velocity than observed for $\beta = 0.500$.

Aiming at complementing the analysis, two points in the diagram presented in Fig. 5 are chosen for the analysis of the time-histories. The yellow point was placed inside the region of bounded results that appears immersed on the instability region. The second point has the same dimensionless frequency ρ but with a different amplitude Δ is also considered inside the region of unbounded solutions. This second point is highlighted in red in Fig. 5.

The time-histories related to these two points are obtained using the Runge-Kutta method implemented in the ode45 function in MATLAB®. The total simulation time is taken as $\tau = 1000$ and the time-step was 10^{-2}. The temporal series associated with the parameters that define the point highlighted in yellow can be seen in the Figure 6.

The red point is put outside the region of unbounded results. Is taken the pair of coordinates ($\rho = 25.8$ and $\Delta = 43.5$) and is created the temporal series using the same criteria of used to the yellow point. The temporal series of the red point can be seen in the Figure 7. The analyzes of temporal series permit verify that the sub-region of stability result in a damping response. It's a simple investigation, but make possible to confirm that the stability diagrams represent correctly what's happen in each pair of coordinates.

CONCLUDING REMARKS

This paper presented the methodology and results regarding the dynamics of two rigid and articulated pipes subjected to simultaneous internal flow excitation and vertical harmonic motion applied to the support. Stability maps of the linearized mathematical model are obtained using the Floquet Theory. As shown, for the range of internal flow velocities herein investigated, the increase in U^* enlarged the regions in the plane of parameters that define the imposed motion in which bounded responses are observed. Additionally, it was showed that the increase in dimensionless mass β gave rise to sub-regions of stability inside regions characterized by unbounded responses. Further works include analyses of non-linear model, which allows obtaining post-critical oscillation amplitudes.

ACKNOWLEDGMENTS

Dr. Renato Orsino is grateful for his valuable discussions. The second author is grateful to the Brazilian National Council of Research (CNPq) for the grant 310595/2015-0.

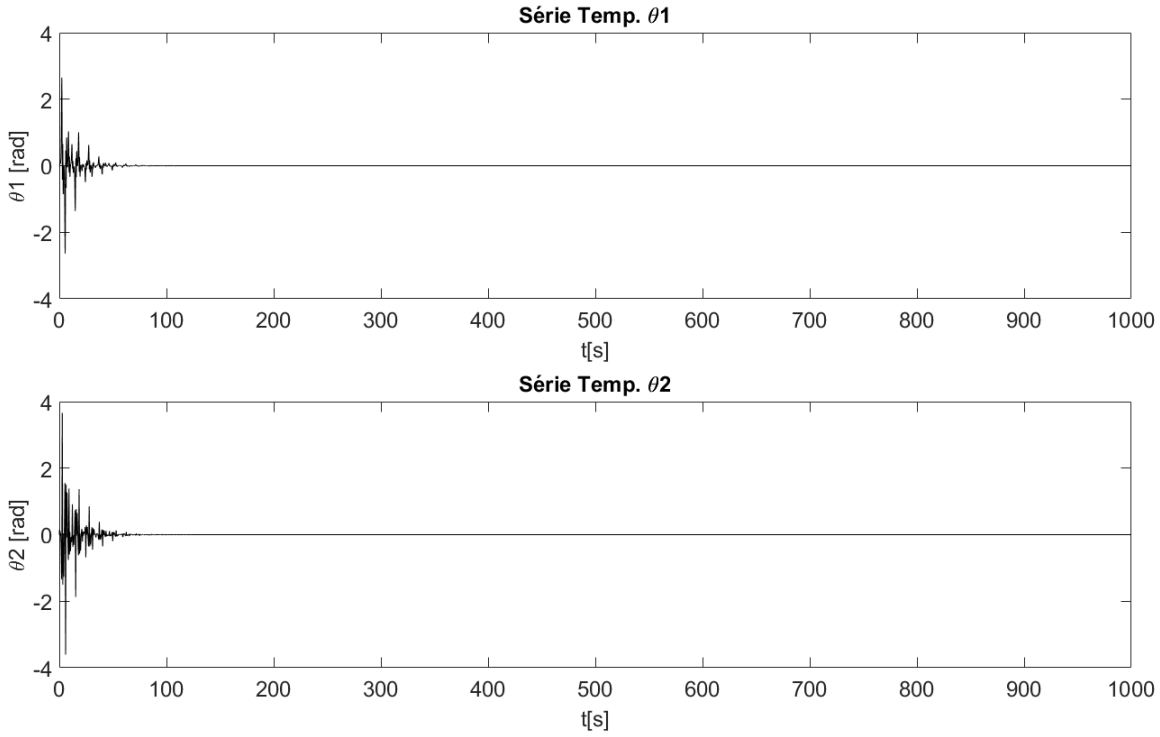

Figure 6 – Temporal series for $\rho = 25.8$ and $\Delta = 54.0$.

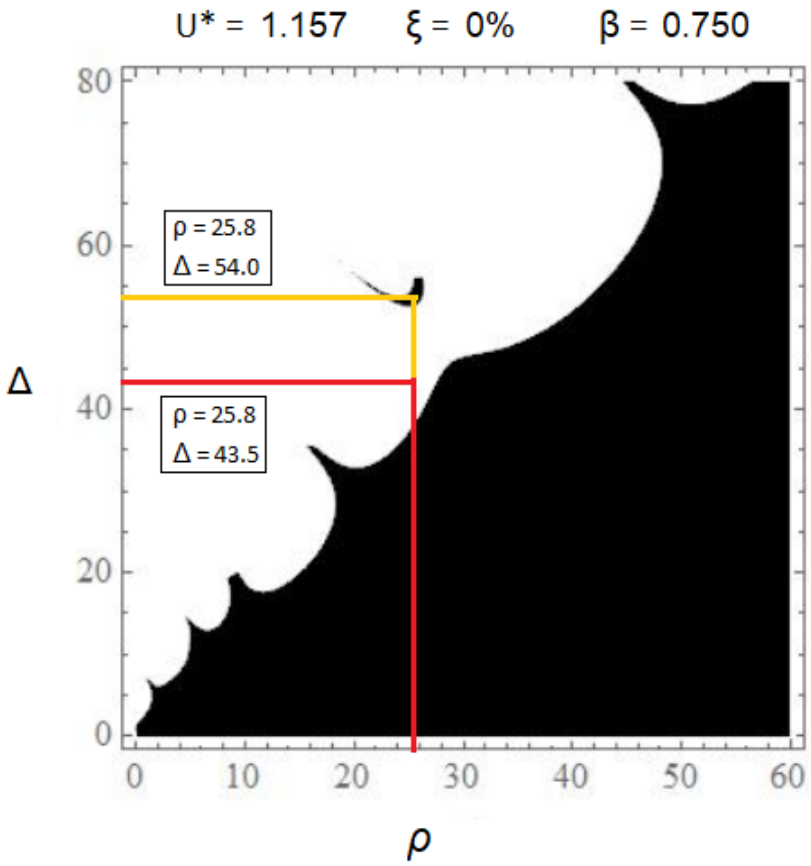

Figure 5 – Stability diagram.

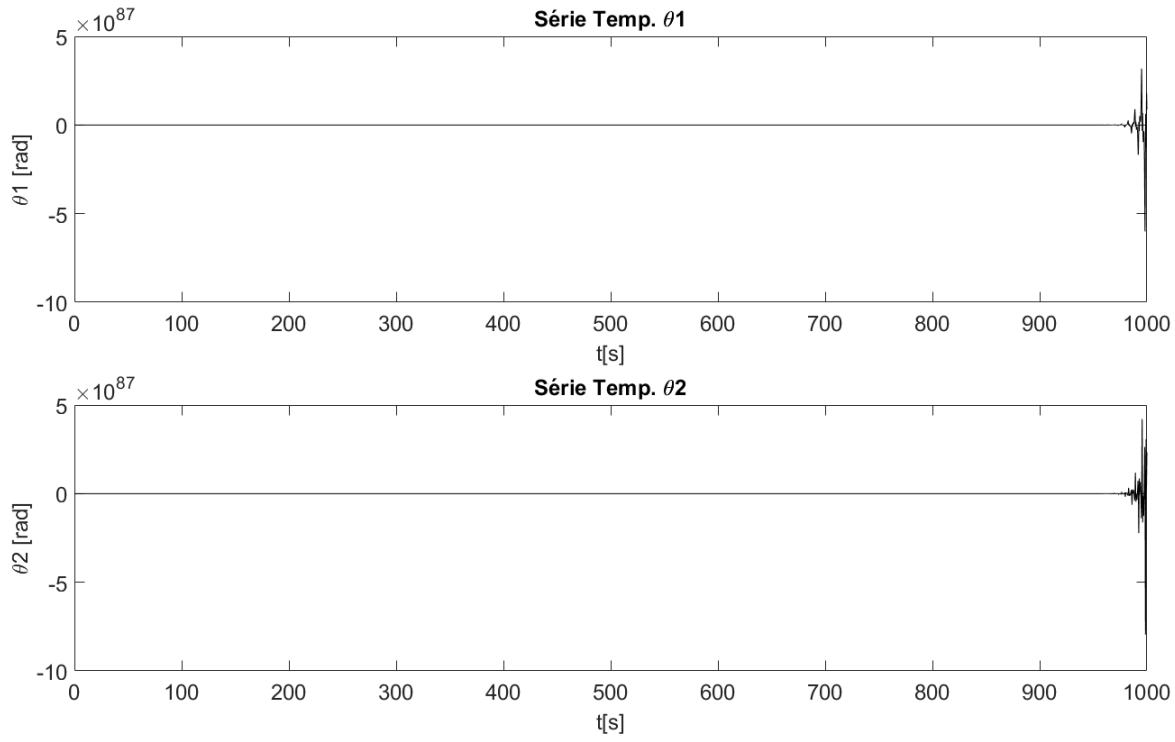

Figure 7 – Temporal series for $\rho = 25.8$ and $\Delta = 43.5$.

REFERENCES

Benjamin, T.B., 1961, "Dynamics of a system of articulated pipes conveying fluid. i. theory.", The Royal Society, Vol.261, No. 1307, pp. 457–486.

Nayfeh, A.H. and Mook D.T., 1979, "Nonlinear oscillations.", Ed. John Wiley and Sons.

Meirovitch, L., 2003, "Methods of Analytical Dynamics.", Ed. McGraw-Hill Book Company.

Orsino, R.M.M. and Pesce C.P., 2018, "Reduced order modeling of a cantilevered pipe conveying fluid applying a modular methodology.", International Journal of Non-Linear Mechanics, Vol. 103, pp. 1–11

Orsino, R.M.M., Pesce C.P. and Franzini, G.R., 2017, "Cantilevered pipe ejecting fluid under VIV: Non-linear reduced order modeling and analysis", Procceedings of the 24th ABCM International Congress of Mechanical Engineering.

Orsino, R.M.M., Pesce C.P. and Franzini, G.R., 2018, "A 3D Non-Linear reduced order model for a cantilevered pipe conveying fluid under VIV", Procceedings of the 9th International Symposium on FIV Flow-Induced Vibration and Noise.

Païdoussis, M.P., 1998, "Fluid-Structure Interactions - slender structures and axial flow Volume 1", Ed. Academic Press.